

# Lawrence Berkeley National Laboratory

Lawrence Berkeley National Laboratory

## Title

Numerical study of the THM effects on the near-field safety of a hypothetical nuclear waste repository - BMT1 of the DECOVALEX III project. Part 3: Effects of THM coupling in sparsely fractured rocks

## Permalink

<https://escholarship.org/uc/item/86t7c2w8>

## Authors

Rutqvist, J.  
Chijimatsu, M.  
Jing, L.  
et al.

## Publication Date

2004-09-09

Peer reviewed

Numerical Study of THM Effects on the Near-field Safety of a Hypothetical Nuclear Waste Repository – BMT1 of the DECOVALEX III Project. Part 3: Effects of THM coupling in sparsely fractured rocks

Version 6  
September 9, 2004

J. Rutqvist<sup>a</sup>

M. Chijimatsu<sup>b</sup>

L. Jing<sup>c</sup>

A. Millard<sup>d</sup>

T.S. Nguyen<sup>e</sup>

A. Rejeb<sup>f</sup>

Y. Sugita<sup>g</sup>

C.F. Tsang<sup>a</sup>

a. Lawrence Berkeley National Laboratory (LBNL), Berkeley, USA

b. Hazama Corporation, Tokyo, Japan

c. Royal Institute of Technology (KTH), Stockholm, Sweden

d. Commissariat a l'Energie Atomique (CEA), Paris, France

e. Canadian Nuclear Safety Commission (CNSC), Ottawa, Canada

f. Institut de Radioprotection et de Sûreté Nucléaire (IRSN), Paris, France

g. Japan Nuclear Cycle Development Institute (JNC), Ibaraki, Japan

## ABSTRACT

As a part of the international DECOVALEX III project, and the European BENCHPAR project, the impact of thermal-hydrological-mechanical (THM) couplings on the performance of a bentonite-back-filled nuclear waste repository in near-field crystalline rocks is evaluated in a Bench-Mark Test problem (BMT1) and the results are presented in a series of three companion papers in this issue. This is the third paper with focus on the effects of THM processes at a repository located in a sparsely fractured rock. Several independent coupled THM analyses presented in this paper show that THM couplings have the most significant impact on the mechanical stress evolution, which is important for repository design, construction and post-closure monitoring considerations. The results show that the stress evolution in the bentonite-back-filled excavations and the surrounding rock depends on the post-closure evolution of both fields of temperature and fluid pressure. It is further shown that the time required to full resaturation may play an important role for the mechanical integrity of the repository drifts. In this sense, the presence of hydraulically conducting fractures in the near-field rock might actually improve the mechanical performance of the repository. Hydraulically conducting fractures in the near-field rocks enhances the water supply to the buffers/back-fills, which promotes a more timely process of resaturation and development of swelling pressures in the back-fill, thus provides timely confining stress and support to the rock walls. In one particular case simulated in this study, it was shown that failure in the drift walls could be prevented if the compressive stresses in back-fill were fully developed within 50 years, which is when thermally induced rock strain begins to create high differential (failure-prone) stresses in the near-field rocks.

# 1 INTRODUCTION

This paper evaluates the impact of thermal-hydrological-mechanical (THM) couplings on the performance of a bentonite-back-filled nuclear waste repository in a sparsely fractured hard rock. The present paper is the third of three companion papers on Bench Mark Test 1 (BMT1) of the DECOVALEX III and BENCHPAR projects [1]. The overall aims and definition of the BMT1, as well as the model conceptualization and characterization, were presented in the first companion paper [2]. The second companion paper [3] focused on the impact of THM coupling for a repository located in continuous and homogeneous (intact) rock without fractures. This is the third (and final) paper with focus on the impact of THM couplings in near-field of a repository located in sparsely fractured rock (Fig. 1b). The sparsely fractured rock in this case is envisioned as a fractured rock mass that contains a few connected hydraulically conducting fractures that carry the main part of the water flow. In this case, one vertical fracture is assumed to be located about 5 m from the deposition hole, and this fracture is connected to another horizontal fracture that intersects the deposition hole (Fig. 1b). The results and conclusions are based on coupled THM analyses conducted by four research teams: Royal Institute of Technology (KTH), Canadian Nuclear Safety Commission (CNSC), Commissariat à l'Énergie Atomique de Cadarache (CEA), and Japan Nuclear Fuel Cycle Development Institute (JNC). Computer codes used by each research team and their sources [4, 5, 6, 7] are listed in Table 1.

In this paper, we will first introduce briefly the simulation tasks and model conceptualisations. The THM model conceptualisations and simulation results are then

presented, followed by discussions about the impacts of THM couplings and near-field rock fractures on repository performance. The impact of fractures is analysed by a comparison with results in the second accompanying paper on continuous homogeneous (intact) rock [3].

## **2 SIMULATION TASKS**

The basic task of BMT1 was to perform a scoping calculation of coupled THM processes around a hypothetical bentonite-back-filled nuclear waste repository in fractured rock. The repository geometry is based on the radioactive waste disposal concept from the Japanese H12 project [8]. Using this concept, the spent-fuel assemblies will be encapsulated in metal canisters, then placed in vertical deposition holes drilled from horizontal drifts deep in the bedrock. The waste canisters are embedded in a buffer of a highly compacted bentonite-based material, and the drifts are back-filled with a mixture of bentonite, sand, and crushed rock (Fig. 1b). This is similar to prospective designs and engineering barrier systems for many countries [9], including the original Swedish KBS-III concept. Most of the material properties for buffer and rock were extracted from a comprehensive data set that was been developed at the Kamaishi Mine, Japan, during DECOVALEX II. Additional rock properties are taken from data sets of the sparsely fractured crystalline in the Canadian Shield.

The overall objective of BMT1 is to investigate the impact of coupled THM processes on the near-field performance of a typical bentonite-back-filled nuclear waste repository. To investigate the influence of each coupling mechanism, the results of a fully coupled THM

simulation is compared to partially coupled solutions. Four simulations are therefore conducted. First, a fully coupled THM simulation is conducted, including the most apparent couplings illustrated in Fig. 2. Thereafter, coupled TH/uncoupled M, coupled HM/uncoupled T, and coupled TM/uncoupled H simulations are conducted. In these simulations, one of the processes M, T or H was uncoupled, meaning that these processes are solved independently of the others. However, all simulations start with the same initial conditions (before excavation for the rock and after emplacement for the bentonite). For example, when running coupled TH/uncoupled M simulations, the hydraulic conductivity of the rock is determined by the initial effective stress and is kept constant throughout the simulation. In the case of coupled HM/uncoupled T simulations, the thermal conductivity of the bentonite is independent of water saturation and is therefore set to the thermal conductivity at the initial saturation, which is 65%. Finally, for coupled TM/uncoupled H simulations, the hydraulic simulation is conducted independently of the T and M responses which implies that the hydraulic conductivity is constant and that a specific storage coefficient has to be estimated.

For guidance concerning the effect of THM on the performance of a repository, a number of performance measures were defined (see [2]). This includes the evolution of temperature in the buffer and associated maximum temperature, the evolution of moisture in the buffer and associated time to full resaturation, and the evolution of stress in the buffer and rock and associated possibility of rock failure. The evolution of temperature and saturation are important for the assessment of performance of the bentonite buffer. In general, the maximum temperature should not exceed 100°C, since higher temperatures

might induce unwanted chemical changes to the bentonite. The resaturation process is expected to take place uniformly to ensure that the bentonite swells uniformly to prevent high and uneven stressing of the waste canister. The stress evolution in both back-fill and rock is important for the structural integrity of the host rock. Any structural changes in the host rock might affect the drift stability or rock mass transport properties. Those changes should be quantified to assess their impact on the performance of the repository as a whole. By performing the coupled THM analysis of the hypothetical repository, and by comparing the results for fully coupled THM analysis with partially coupled TH, HM, and TM analyses, the impact of the various coupling on the performance measures are evaluated.

### **3 MODEL CONCEPTUALIZATION**

Because of preoic nature of the repository concept design, the simulations were conducted with an one-quarter symmetric model containing one deposition hole (Fig. 3). The upper and lower boundaries are placed at vertical distances of 50 m from the drift floor, according to the BMT1 definition [2]. A vertical fracture located between two adjacent drifts (Fig. 1b) is connected to the constant pressure boundaries on the top and bottom of the model. The vertical fracture connects to a horizontal fracture that intersection the deposition hole. The exact dimensions of canister, deposition hole, and drifts are given in the first companion paper [2].

Most of the material properties for the bentonite-based buffer, back-fill, and rock were extracted or developed during DECOVALEX II for modelling of the Kamaishi Mine

heater test [10]. Properties for the bentonite-based buffer material were further calibrated in the first companion paper [2] for improved model representation of *in situ* THM responses at Kamaishi Mine. In general, the buffer material used in this simulation is a bentonite-sand mixture with a saturated permeability of  $1.6 \times 10^{-20} \text{ m}^2$ , a porosity of 40%, a thermal conductivity varying from  $0.5 \text{ W/m}\cdot\text{C}$  (dry) to  $1.2 \text{ W/m}\cdot\text{C}$  (wet), a dry specific heat of  $426 \text{ J/kg}\cdot\text{C}$ , a Young's modulus of the order of 0.03 to 0.1 GPa, and a moisture swelling stress of about 1 MPa. Typical saturation dependent functions for water retention, diffusion coefficients and swelling stress used for this buffer material are shown in Rutqvist et al. [10] (see Fig. 3). The rock matrix represents an intact granite with a permeability varying between  $1 \times 10^{-19}$  and  $1 \times 10^{-17} \text{ m}^2$ , a porosity of 0.4%, a thermal conductivity of  $2.7 \text{ W/m}\cdot\text{C}$ , a specific heat of  $833 \text{ J/kg}\cdot\text{C}$ , a density of  $2746 \text{ kg/m}^3$ , a Young's modulus of 60 GPa, and a thermal expansion coefficient of  $8 \times 10^{-6} \text{ 1/C}$ . A Biot's parameter  $\alpha$  for the intact rock varies between 0.2 to 1.0 between models by different teams (see companion second paper [3], Table 2). The back-fill for the drifts consists of a bentonite-sand-rock mixture with properties extracted from the Japanese H12 report [8]. This back-fill material is generally more permeable ( $k = 6.0 \times 10^{-19} \text{ m}^2$ ) than the buffer material, and the swelling stress is only about 0.2 MPa.

The mechanical and hydro-mechanical properties of the horizontal rock fracture were estimated using the Barton-Bandis' Joint model [11]. In this context, the void aperture,  $b_v$ , is defined as the accessible volume per unit area of a fracture. The void aperture at a given effective normal stress is

$$b_v = b_{vr} + \Delta b_v \quad (1)$$



where  $b_{vr}$  is a residual void aperture when the fracture is completely compressed from a mechanical point of view, and  $\Delta b_v$  is mechanically induced void aperture for an incompletely compressed fracture during a deformation process.

The mechanically induced void aperture can be related to the current effective normal stress,  $\sigma'_n$ , using Barton-Bandis' hyperbolic normal closure model according to

$$\Delta b_v = \frac{k_{n0} V_{m0}^2}{\sigma'_n + k_{n0} V_{m0}} \quad (2)$$

where  $k_{n0}$  and  $V_{m0}$  are, respectively, the normal stiffness and maximum normal closure at the zero stress intercept [11]. The parameters  $k_{n0}$  and  $V_{m0}$  were estimated using the basic parameter values  $JRC_0 = 9$ ,  $JCS_0 = 105$  MPa and  $\sigma_{ci} = 123$  MPa (extracted from the Kamaishi Mine data set). Using formulas presented in Barton and Bakhtar [11],  $k_{n0} = 56$  GPa/m and  $V_{m0} = 65$   $\mu\text{m}$  were derived for the fourth loading cycle.

For the hypothetical case presented in this analysis, we assume  $b_h = 0.85 \times b_v$ , where  $b_h$  is the hydraulic aperture defined from the parallel plate flow relationship

$$T_f = \frac{b_h^3 \rho g}{12\mu} \quad (3)$$

Fig. 4 presents the resultant relationship between the fracture transmissivity and effective normal stress. This function represents a fracture whose initial aperture is 10  $\mu\text{m}$  at an initial effective stress of 17 MPa, corresponding to the initial vertical effective stress across the horizontal fracture that intersects the deposition hole.

The mechanical integrity of the rock mass is estimated using Hoek and Brown's failure criterion, which can be written as [12]:

$$\sigma'_1 = \sigma'_3 + \sigma_{ci} \left( m_b \frac{\sigma'_3}{\sigma_{ci}} + s \right)^a \quad (4)$$

where  $\sigma'_1$  and  $\sigma'_3$  are the maximum and minimum principal compressive effective stresses at failure, respectively,  $m_b$  is the value of the Hoek-Brown constant  $m$  for the rock mass,  $s$  and  $a$  are constants that depend upon the characteristics of rock mass, and  $\sigma_{ci}$  is the uniaxial compressive strength of the intact rock pieces. In this simulation, the empirical constants have been estimated as  $a = 0.5$ ,  $m_b = 17.5$  and  $s = 0.19$ , which represents a very good quality rock mass of sparsely fractured granite.

#### 4 MODELING SEQUENCES AND BOUNDARY CONDITIONS

Fig. 5 presents the modeling sequence, and boundary and initial conditions for the coupled THM simulation. The initial conditions for the rock mass are defined at the pre-excavation stage (Fig. 5a). The temperature is assumed to be 45°C over the entire 100 m high model column, while the pore pressure and stress increase with depth. Because the effective stress increases with depth, the initial permeability decreases with depth depending on the assumed stress- permeability relation. The excavation sequence was simulated in an one-step steady-state calculation with the elements in the drift removed (Fig. 5b). In this simulation, the pressure and temperature in the drifts were reduced to 0 MPa and 20°C, respectively. The rock around the drift was cooled from the initial temperature of 45°C down to 20°C, and induced significant thermal-mechanical effects. After the steady-state excavation simulation was completed, the waste canister, bentonite

buffer, and back-fill were installed instantaneously and the post-closure simulation starts (Fig. 5c and 5d). The post-closure simulations were conducted for up to 1,000 years, when the ambient temperature and fluid pressure fields were reestablished.

## 5 THM SIMULATION RESULTS

Fig. 6 summarises the general results of THM analyses by teams of CEA, CNSC, KTH, and JNC. Calculated results of time evolutions of temperature, water content, pore pressure and stress at selected points (B4 in the buffer and R1 in the rock) are shown in Fig. 7 and 8.

The calculated results summarised in Fig. 6 includes coupled THM effects of typical thermally-driven coupled processes that have also been observed at several *in situ* heater tests in bentonite-rock systems, including the Kamaishi Mine and the FEBEX *in situ* experiments [13, 14]. The main coupled THM processes illustrated in Fig. 6a are: 1) evaporation of liquid water to vapor near the waste canister, 2) transport of vapor by thermally induced diffusion by the thermal gradient away from the canister toward cooler regions, 3) condensation of vapor to liquid water in cooler regions of the buffer close to the rock-buffer interface, 4) capillary-driven infiltration of liquid water from the fully saturated rock into the partially saturated buffer, 5) temporal drying and associated drying shrinkage of the bentonite near the waste canister during the first few years, 6) swelling of the bentonite-based buffer as a result of incipient wetting at the rock-buffer interface and slowly progressing toward the interior of the buffer, 7) restoration of hydrostatic fluid pressure in the near-field rock and buffer with associated changes in the stress field, and 8) thermally induced strain with associated stress and deformations in both the buffer and

surrounding rock. These thermally driven coupled processes are significant as long as the temperature in the waste canister is significantly different from the ambient temperature (until about 400 years in this case). After 400 years, the ambient temperature is almost re-established, the buffer is fully saturated, a hydrostatic fluid pressure gradient from the ground surface has been restored, and the compressive stresses in the buffer are fully developed (Fig. 6b).

Fig. 7a shows that the maximum temperature of about 75 to 80°C is reached at the surface of the waste canister after about 30 to 40 years. The slightly lower peak temperature obtained by CNSC may be related to a lower initial temperature. At 1,000 years, the heat power is down to a few percent of its initial value and the temperature has declined to about 48 to 50°C, which is a few degrees above ambient temperature.

Fig. 7b shows that the time to full resaturation of the buffer varies between 3 to 10 years according to the calculations made by the various teams. The different resaturation times among these models are in line with simulation results obtained for the well-defined axisymmetric problem [2] and for the case of a homogenous (intact) rock [3]. This indicates that the variation of the resaturation times among these models are caused by slightly different input hydraulic properties of the buffer, such as relative permeability and water-retention curves. After the buffer has been fully resaturated with water, the liquid fluid pressure becomes positive (in unsaturated media, the liquid fluid pressure is generally negative), and a fully restored hydrostatic fluid pressure is achieved after a few additional years.

The simulated evolution of compressive stress in the buffer is very similar between CEA and KTH models, whereas CNSC model obtained a substantially higher compressive stress (Fig. 7c). In the results achieved with CEA and KTH models, the bentonite provides a swelling stress (which is an effective stress) of about 1 MPa. The remaining 10 MPa of the total compressive stress in the buffer is caused by the contribution from the fluid pressure, which increases from 0 to a hydrostatic value of 10 MPa at a depth of 1,000 meters. Thus, the results indicate that the impact of the fluid-pressure restoration is a dominant component contributing about 90% of the total compressive stress in the buffer.

Fig. 8 presents the KTH results for the evolution of stress in the rock at point R1 at a critical location for the evaluation of rock failure. As shown in the second companion paper [3], the highest potential for rock failure occurs on the floor of the drift. Fig. 8a shows that the maximum compressive principal effective stress,  $\sigma'_1$ , is 93 MPa at about 40 years. However, Fig. 8b shows that the risk for rock failure is the highest after excavation and at about 100 years, when the minimum compressive principal effective stress,  $\sigma'_3$ , is relatively small. It can thus be concluded that the evolution of minimum compressive principal stress is the most important factor in determining the state of failure of the rock walls of the deposition hole and the drift.

## **6 IMPACT OF THM COUPLINGS**

Comparisons of partially coupled TH, HM, and TM solutions with a fully coupled THM solution are utilised to study the impact of various couplings. Fig. 9a shows that TH

couplings have a small impact on the temperature field until the buffer is fully saturated. This slight impact is caused by thermal conductivity's dependency on liquid saturation. However, THM couplings have no visible impact on the peak temperature.

Fig. 9b shows a slight difference between HM and THM results, indicating that TH coupling has only a slight impact on the resaturation of the buffer. In TH and THM simulations, the resaturation of the bentonite buffer is slightly delayed because of thermally induced drying near the canister surface. The identical results of TH and THM simulations in Fig. 9b shows that HM coupling has no impact on the resaturation process. This implies that in this case stress-induced changes in fracture permeability do not have significant impact on the resaturation process. Apparently, sufficient water is provided by the conducting fractures regardless of changes in fracture permeability, and the rate of resaturation is controlled by the properties of the back-fill rather than by the properties of the surrounding rock.

Fig. 9c shows that HM coupling has a strong impact on the total stress in the buffer. The total stress developed in the buffer material is dominated by fluid pressure, which at 1,000 m depth amounts to 10 MPa for final hydrostatic conditions. The magnitude of TM-induced stresses in the buffer is less than 1 MPa.

Fig. 10a shows that the TM coupling has a dominant impact on the evolution of the maximum compressive principal stress at point R1. Apparently, the maximum compressive principal stress is determined by the excavation-induced stress concentration

at the drift walls and by the thermally induced stresses, whereas fluid pressure has almost no impact. The evolution of the minimum compressive principal stress is more complex, with some influence from both TM and HM couplings. The evolution of minimum compressive stress from HM simulation shows a steady increase from 15 to about 50 years, when the compressive stress stabilizes at about 5 MPa. As will be explained in details later, this stress increase is a result of resaturation and fluid-pressure restoration in the back-filled drift, which provides a supporting load to the drift walls. Nevertheless, Fig. 10 shows that full THM analysis must be conducted for an appropriate evaluation of the stress evolution in the near field rock.

## **7 IMPACT OF NEAR-FIELD FRACTURES**

A comparison of simulation results for the case of a deposition hole located in homogenous intact rock (Fig. 1a) with the case of a deposition hole located in sparsely fractured rocks (Fig. 1b) shows that the main effect of the fractures in the near-field rock mass is an accelerated resaturation of the buffer, leading to a much shorter resaturation time in fractured rocks. For the case of a homogeneous, intact, low-permeability rock ( $k=1\times 10^{-19}$  m<sup>2</sup>), the time to full resaturation ranged from 40 to 200 years [3]. By introducing hydraulic conducting fractures, the resaturation time is reduced to 3 to 10 years (Fig. 7b).

The impact of fractures is illustrated by the simulation results of KTH model as shown in Fig. 11. For the case of an intact low permeability rock ( $k = 1e-19$  m<sup>2</sup>), desaturation of the rock surrounding the repository delays the resaturation of the buffer (Fig. 11a). As seen in Fig. 11b, no such desaturation of the rock when the nearby fractures are included.

Note that desaturation of the rock surrounding the drift is prevented by the influence of both the vertical and horizontal fractures, because they provide nearby sources of hydrostatic water pressure. Thus, even if no fracture intersected the deposition hole, just the presence of connected hydraulic conducting fractures in the near-field rock would be sufficient to prevent desaturation of the rock. Fig. 11b also indicates an increased resaturation adjacent to the intersecting horizontal fracture. This implies that an intersecting fracture impacts the stress evolution and its spatial distribution in the buffer. However, the overall resaturation of the buffer (and resulting evolution of the swelling pressure) is approximately uniform, with fully developed compressive stress tending to occur first in the buffer of the deposition hole and thereafter in the back-fill of the overlying drift.

Fig. 12 compares the evolution of effective principal stresses for the two cases of a deposition hole located in intact and in sparsely fractured rocks according to the KTH simulations. Fig. 12 shows that the possibility of rock failure could be much greater for the case of intact (low-permeability) rock than for the case of sparsely fracture rock. In the case of intact rock, the minimum compressive stress becomes tensile for the time period between 60 and 300 years (Fig. 12, dashed line). During this time, the possibility for failure in the rock mass is imminent, as demonstrated by the stress path shown in Fig. 12 for the case of intact homogenous rock (dashed line) crosses the Hoek-Brown Failure envelope. From Fig. 12 it can again be concluded that the evolution of minimum compressive principal stress is the most important factor for determining the risk for failure at rock walls of the deposition hole and the drift.



The higher possibility of rock failure in the case of intact rock can be explained by the delayed evolution of resaturation in the buffer, as shown in Fig. 11. The delayed resaturation results in a subsequent delay in fluid-pressure restoration, and consequently a delay in the development of compressive stress in the buffer. When fractures are present in the near-field rock, on the other hand, the accelerated resaturation process results in an accelerated development of compressive stresses in the buffer and the back-fill. This implies that when hydraulic conducting fractures are present in the near-field rock, the compressive stress in the buffer and back-fill develops within 15 of 50 years, respectively. The increased compressive stress in the buffer and the back-fill provides support and confining stress to the rock surfaces, therefore tends to stabilise the rock walls. Fig. 13 illustrates the support stress from the buffer and back-fill on the excavation walls and its impact on minimum compressive principal stress at point R1 on the floor of the drift. In general, minimum compressive principal effective stress is directed normal to the drift walls, and in this case, normal to the floor of the drift. The support pressure, provided by the back-fill on the drift floor after full resaturation, fully restored hydrostatic fluid pressure, and the re-established ambient temperature could be estimated as  $\sigma_{wall} = \sigma_{sw} + P_w \approx 0.2 + 10 = 10.2$  MPa (the swelling pressure,  $\sigma_{sw}$ , is only on the order of 0.2 MPa in the back-fill). The resulting minimum compressive effective stress in the drift wall is then  $\sigma'_3 = \sigma_{wall} - \alpha P_w \approx 10.2 - 0.5 \cdot 10 = 5.2$  MPa ( $\alpha = 0.5$  in the simulation by KTH). This is close to the values of the minimum compressive principal stress at the point marked “final” in Fig. 12. However, during the heating phase, the evolution of minimum compressive principal stress also impacts the evolution of thermal stresses, as

shown in the sinusoidal cyclic behaviour in Fig. 8a and 10b. As shown in Fig. 10b, this cyclic behaviour occurs for both TM and THM analysis, but in the case of THM analysis, the curve is shifted (about 5 MPa) toward more the compressive stress direction. This shift is caused by the support pressure from the back-fill on the drift wall, as illustrated in Fig. 13. Because the minimum compressive principal stress tends to go into tension at about 60 years, the fully developed compressive stress at about 50 years effectively prevents failure in this case.

The results shown in Fig. 12 were calculated by the KTH team. The simulation results of the other three teams also show that the potential for failure is a result of complex interaction among coupled THM processes in both the back-fill and rock. Although all teams found a potential for failure, the exact spatial and time evolution varied among the teams. In particular, the CEA and CNSC teams found a potential for failure only at excavation, and not at later times. These differences were caused by the difference in calculated resaturation time, and corresponding difference in calculated evolution of swelling pressure, as well as by a difference in the value for Biot's  $\alpha$  assigned to the various models. Most notably, the resaturation time for CEA and CSNC was less than 20 Years even for the intact rock case [3], and therefore rock failure could be prevented at later times in those simulations. A variation of Biot's  $\alpha$  between 0.2 and 1 can also be important, with a much higher likelihood for failure if  $\alpha$  is close to 1 rather than 0.2 (see equations in Fig. 13).

## **8 DISCUSSION**

The studies on BMT1 of the DECOVALEX III projects have helped to reveal some outstanding issues related to predicting coupled THM processes in the engineered barrier system and surrounding fractured rock. In particular, the studies presented in these three companion papers have shown that the buffer resaturation and fluid-pressure restoration processes could be important for the stability of the rock walls, both for the deposition holes and the drifts. A timely resaturation would assure a timely development of compressive stress in the buffer and back-fill, which provides a timely support load on the rock walls of deposition holes and drifts. However, several *in situ* tests (e.g., Kamaishi Mine heater test, FEBEX *in situ* test) indicate that the resaturation of the buffer may be delayed because of the micro-structural behavior of bentonite, which can effectively substantially decrease permeability as a result of swelling of microparticles. As shown in this paper, a delay in the resaturation and fluid-pressure restoration in the buffer may jeopardize the mechanical stability of excavation walls after closure of the repository. It should also be noted that *in situ* tests are usually conducted in drift under drained conditions, where the fluid pressure remains much lower than the re-established hydrostatic pressure that might be present at a future repository located at 500 to 1,000 meters depth.

## **9 SUMMARY AND CONCLUSION**

This analysis aimed to evaluate the impact of THM couplings on the performance of a repository located in a sparsely fractured rock under the conditions studies in BMT1. The results of this analysis can be summarised as follows:

- **Temperature evolution (T process) :** No significant effect by H and M coupling (conduction dominates).
- **Resaturation of the buffer (H process) :** Affected by T coupling but not significantly by M coupling.
- **Stress evolution in the buffer (M process):** Strongly affected by H coupling and slightly affected by T coupling.
- **Stress evolution in rock for stability and design considerations (M process):** Strongly affected by both T and H coupling.

It is clear that temperature can be predicted accurately without consideration of coupling to hydraulic and mechanical processes. It is also clear that mechanical behaviour—that is, evolution of stress in the buffer-rock system—cannot be appropriately predicted without consideration of effects of temperature and fluid pressure evolutions. It is not clear for the BMT1 case, however, at this point whether the hydraulic behaviour (for example, resaturation of the buffer and radioactive nuclide transport) can be significantly impacted by T and M processes. For the parameter set adopted in this analysis, the resaturation process is slightly impacted by the effect of temperature, whereas that process is not significantly impacted by mechanically induced changes in permeability.

The general results concerning the impact of various THM couplings for a deposition hole located in sparsely fractured rock are generally in line with those of a homogenous (intact) low-permeability rock [3]. The main difference is that hydraulic conducting fractures provide an additional water supply that prevents desaturation of the rock and accelerates the resaturation of the buffer and back-fill.

This analysis shows that a rapid resaturation and development of the swelling stress in the buffer could be beneficial to the mechanical stability of the drift walls. If hydraulic conducting fractures are present in the near-field rock, then buffer and back-fill will be readily resaturated, which results in a timely development of compressive stress in the buffer and back-fill. A timely development of compressive stress in the buffer and back-fill provides confining stress and support to the drift walls before thermal strain creates high differential (failure prone) stresses. The analysis for this particular case indicated that if the buffer and back-fill are fully saturated, and if fluid pressure is fully restored before 50 years, then rock failure in the drift wall would be prevented.

## **ACKNOWLEDGEMENTS**

The following organisations are gratefully acknowledged for their financial support (alphabetical order): the Canadian Nuclear Safety Commission; the Commissariat à l'Énergie Atomique; the European Commission through the BENCHPAR project under Contract FIKW-CT-2000-00066; the Institut de Radioprotection et de Sûreté Nucléaire; the Japan Nuclear Fuel Cycle Development Institute, the Swedish Nuclear Power Inspectorate.

## **REFERENCES**

- [1] Tsang C-F. et al., *Int. J. Rock Mech. Min. Sci.* (This issue) 2004.
- [2] Chijimatsu M, Nguyen TS, Jing L, De Jonge J, Kohlmeier M, Millard A, Rejeb A, Rutqvist J, Souley M, Sugita Y. Numerical study of the THM effects on the near-field safety of a hypothetical nuclear waste repository – BMT1 of the DECOVALEX III project. Part 1: Conceptualization and characterization of the problems and summary of results. *Int. J. Rock. Mech. Min. Sci.* (This issue) 2004.

- [3] Millard A, Rejeb A, Chijimatsu M, Jing L, De Jonge J, Kohlmeier M, Nguyen TS, Rutqvist J, Souley M, Sugita Y. Numerical study of the THM effects on the near-field safety of a hypothetical nuclear waste repository – BMT1 of the DECOVALEX III project. Part 2: Effects of THM coupling in continuous and homogeneous rock. *Int. J. Rock Mech. Min. Sci.* (this issue) 2004.
- [4] Rutqvist J, Börgesson L, Chijimatsu M, Kobayashi A, Nguyen TS, Jing L, Noorishad J, Tsang C-F. Thermohydromechanics of Partially Saturated Geological Media – Governing Equations and Formulation of Four Finite Element Models. *Int. J. Rock Mech. Min. Sci.*, 2001, **38**, 105-127.
- [5] Verpeaux P, Millard A, Charras T., Combescure A. A modern approach of large computer codes for structural analysis. Proc. SmiRT conf., Los Angeles, USA. 1989.
- [6] Nguyen TS. Description of the computer code FRACON. In Stephansson, O., Jing, L., and Tsang, C.-F. editors. *Coupled Thermo-hydro-mechanical Processes of Fractured Media. Developments in Geotechnical Engineering*, Vol 79. Elsevier, Amsterdam, 1996. pp. 539–544.
- [7] Ohnishi Y, Kobayashi A. THAMES. In Stephansson, O., Jing, L., and Tsang, C.-F. editors. *Coupled Thermo-hydro-mechanical Processes of Fractured Media. Developments in Geotechnical Engineering*, Vol 79. Elsevier, Amsterdam, 1996. pp. 545–549.
- [8] Masuda S, Kawata T. The Japanese high-level radioactive waste disposal program. In: Witherspoon PA and Badvarsson GS, editors. *Geological Challenges in Radioactive Waste Isolation: Third Worldwide Review*. Earth Sciences Division, Ernest Orlando Lawrence Berkeley National Laboratory, University of California, LBNL-49767, 2001. pp. 167–182.
- [9] Witherspoon PA, Bodvarsson GS. Introduction to geological challenges in radioactive waste isolation: Third worldwide review. In: Witherspoon PA and Badvarsson GS, editors. *Geological Challenges in Radioactive Waste Isolation: Third World Wide Review*. Earth Sciences Division, Ernest Orlando Lawrence Berkeley National Laboratory, University of California, LBNL-49767, 2001. pp. 1–13.
- [10] Rutqvist J, Börgesson L, Chijimatsu M, Nguyen TS, Jing L, Noorishad J, Tsang C-F. Coupled Thermo-hydro-mechanical Analysis of a Heater Test in Fractured Rock and Bentonite at Kamaishi Mine – Comparison of Field Results to Predictions of Four Finite Element Codes. *Int. J. Rock Mech. Min. Sci.*, 2001, **38**, 129-142.

- [11] Barton NR, Bakhtar K. Rock joint description and modeling for the hydrothermomechanical design of nuclear waste repositories. Technical Report 83-10, TerraTek Engineering, Salt Lake City, Utah, 1983.
- [12] Hoek E, Brown ET. Practical estimates of rock mass strength. *Int. J. Rock Mech. Min. Sci.*, 1997, **34**, 1165–1186.
- [13] Chijimatsu M, Fujita T, Sugita Y, Amemiya K, Kobayashi A. Field experiment, results and THM behaviour in the Kamaishi mine experiment. *Int. J. Rock Mech. Min. Sci.* 2001, **38**, 67–78.
- [14] Alonso E, Alcoverro J, et al. The FEBEX benchmark test case definition and comparison of different modelling approaches. *Int. J. Rock Mech. Min. Sci.* (This issue) 2004.

Table 1. Research teams, codes and their sources

| <b>Acronyme</b> | <b>Research Team</b>                           | <b>Code</b>    |
|-----------------|------------------------------------------------|----------------|
| KTH             | Royal Institute of Technology                  | ROCMAS [4]     |
| CEA             | Commissariat a l'Energie Atomique de Cadarache | Castem2000 [5] |
| CNSC            | Canadian Nuclear Safety Commission             | FRACON [6]     |
| JNC             | Japan Nuclear Fuel Cycle Development Institute | THAMES [7]     |



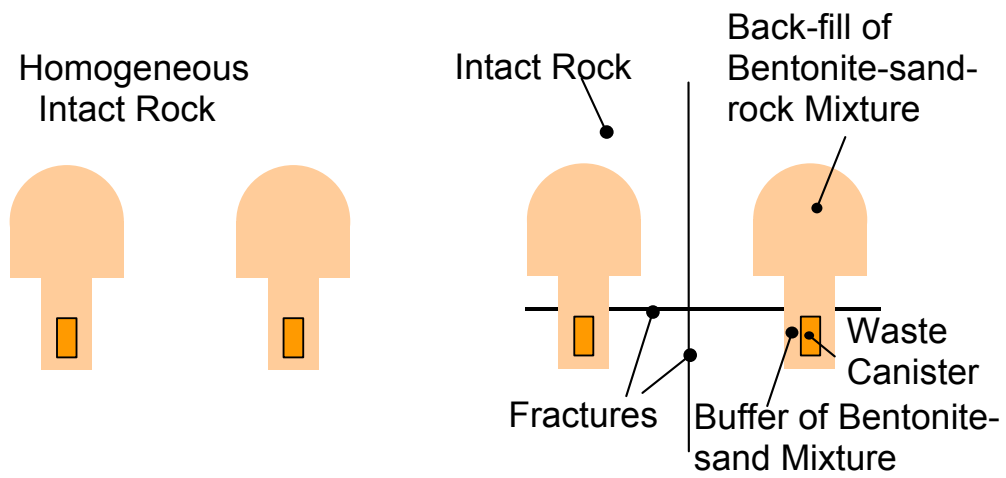
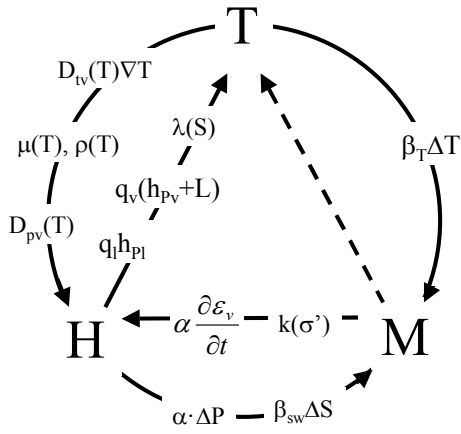


Figure 1. (a) Homogenous intact rock versus (b) sparsely fractured rock cases.



- $D_{Tv}(T)\nabla T$  = Vapor diffusion along thermal gradient
- $\mu(T)$  = Temperature dependent fluid viscosity
- $\rho(T)$  = Temperature dependent fluid density
- $D_{Pv}(T)$  = Temperature dependent vapor diffusion
- $\lambda(S)$  = Saturation dependent thermal conductivity
- $q_v(h_{pv}+L)$  = Heat convection with vapor flow
- $q_i h_{pl}$  = Heat convection with liquid fluid flow
- $\alpha \partial \varepsilon_v / \partial t$  = Poroelastic volume change
- $k(\sigma')$  = Stress dependent permeability
- $\alpha \Delta P$  = Effect of fluid pressure on effective stress
- $\beta_{sw} \Delta S$  = Moisture (saturation) induced strain
- $\beta_T \Delta T$  = Thermal strain

Figure 2. Examples of coupled THM processes considered in this study.

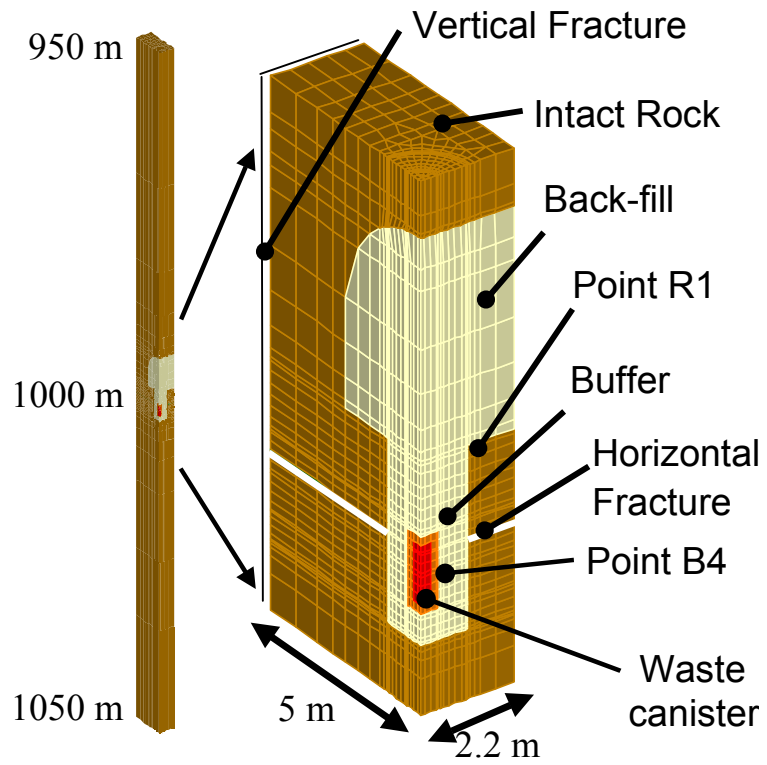


Figure 3. Quarter symmetric model of the hypothetical repository located at 1000 meters depth (KTHs model).

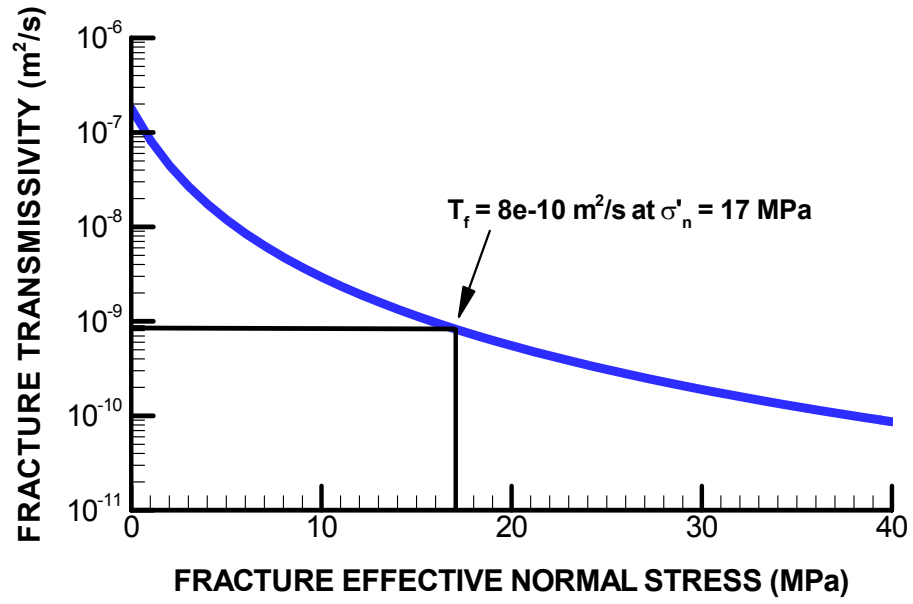
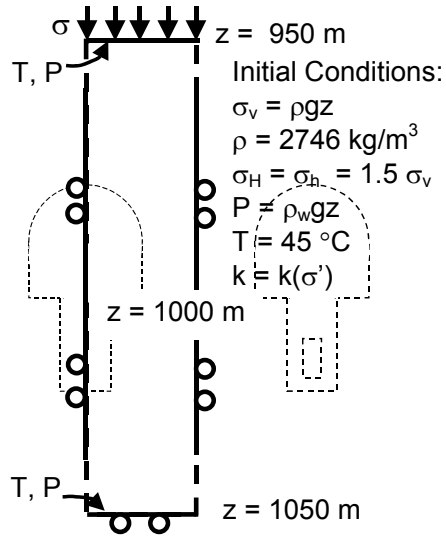
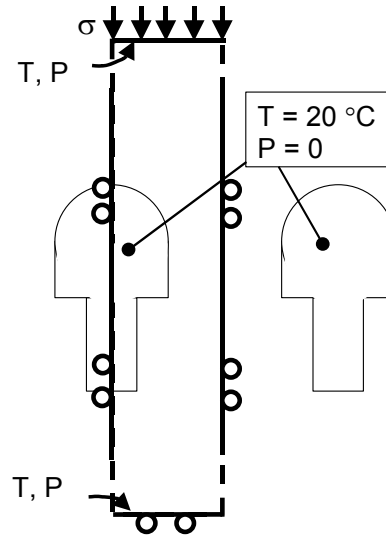


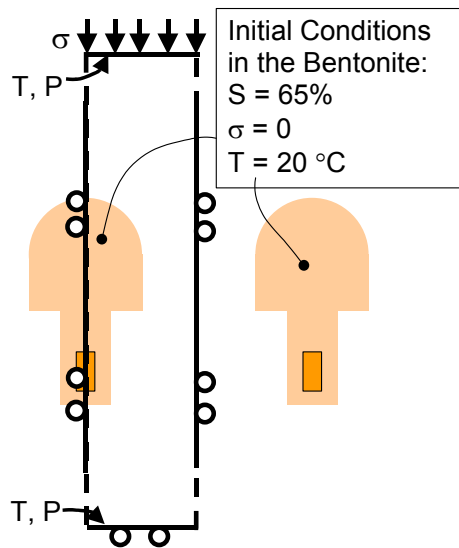
Figure 4. Fracture transmissivity versus effective fracture stress derived for  $k_{n0} = 56$  GPa/m and  $V_{m0} = 65 \mu\text{m}$ .



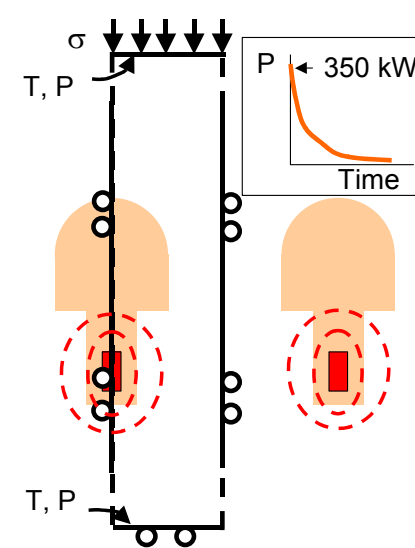
1) Pre-Excavation Conditions



2) Steady State Simulation of Excavation



3) Installation of bentonite



4) Transient simulation of Post-closure

Figure 5. Modeling sequence, boundary and initial conditions for coupled THM simulation.

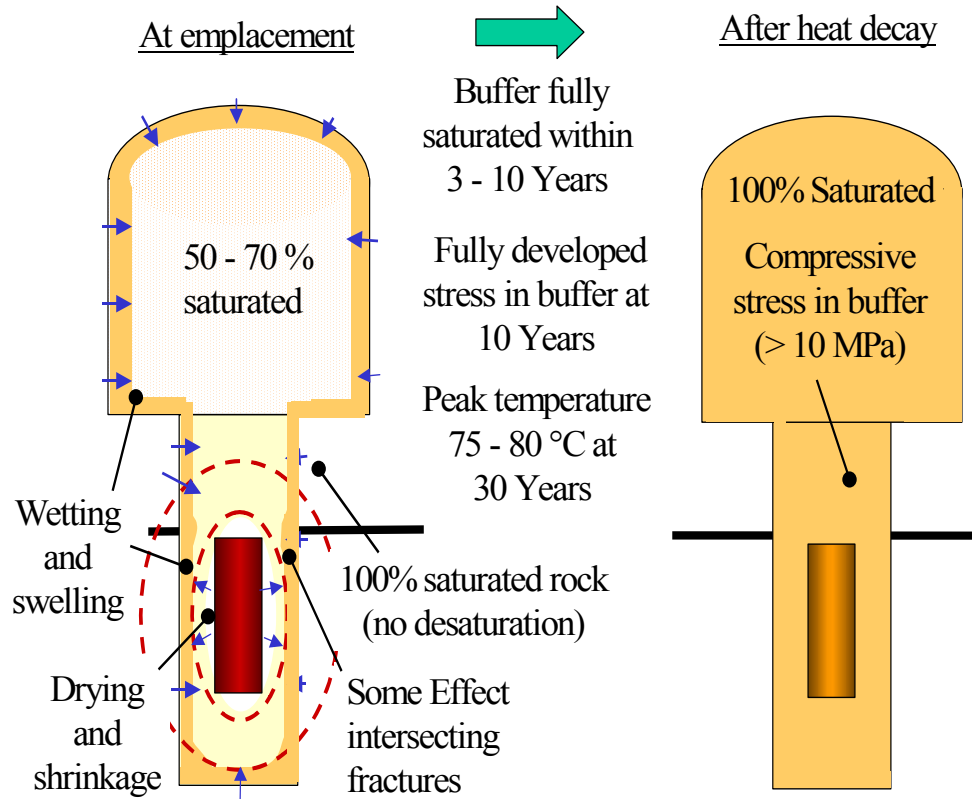
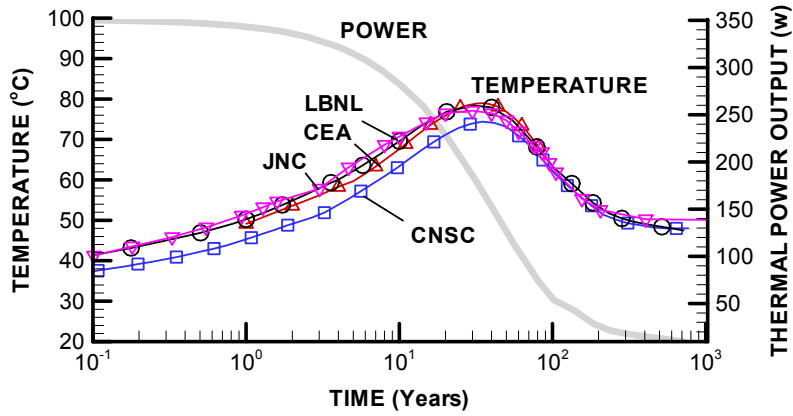
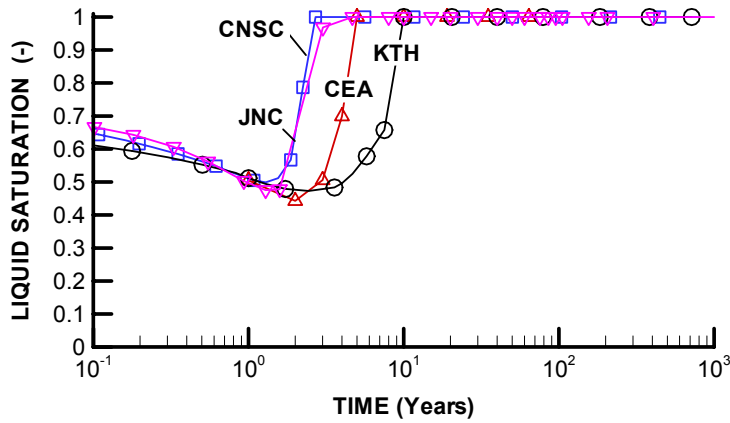


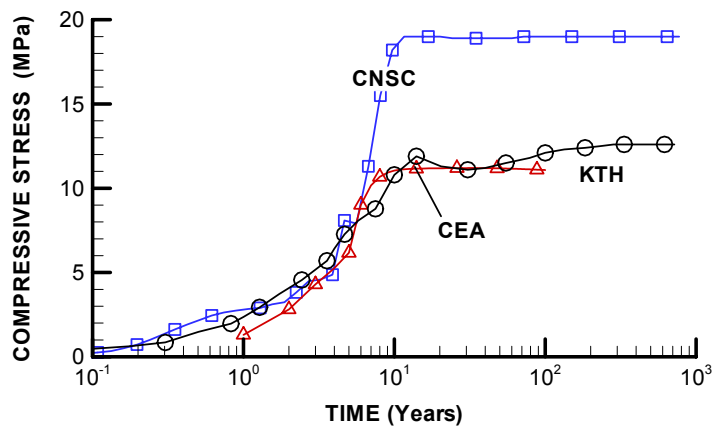
Figure 6. General results from coupled THM simulations of a hypothetical repository in sparsely fractured rock



a) Heat power and temperature evolution

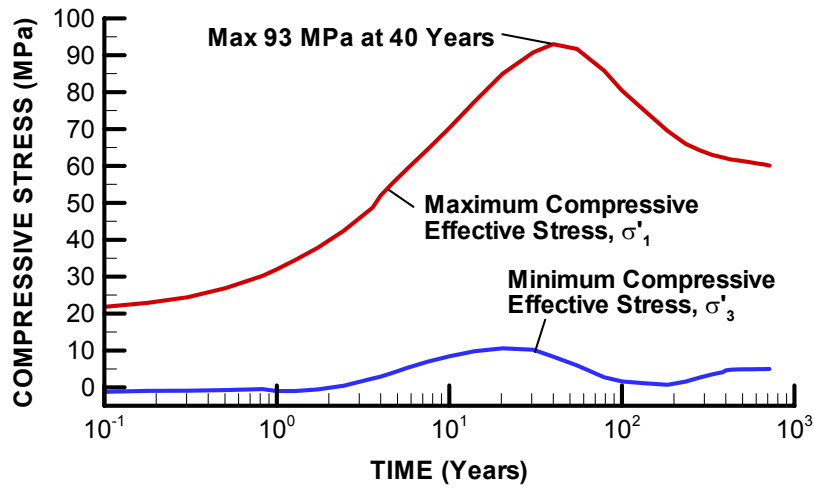


b) Evolution of liquid saturation

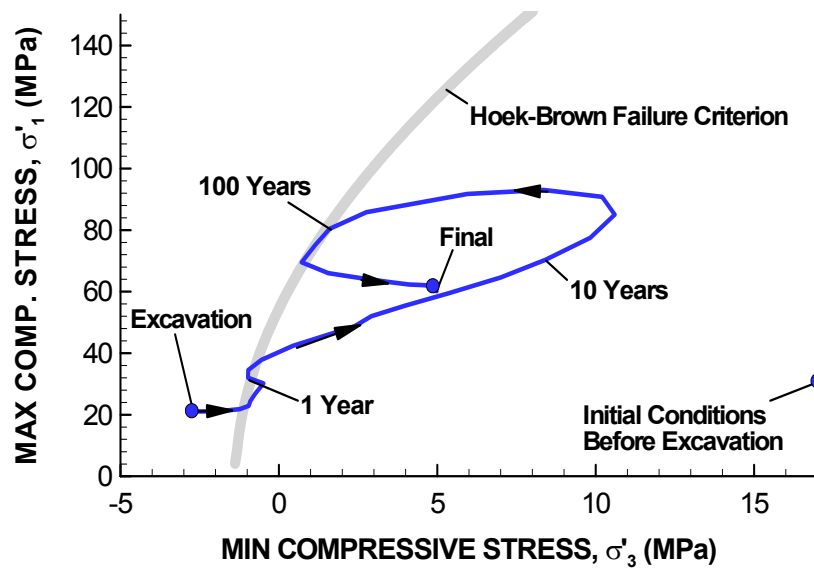


(c) Evolution of compressive stress (total stress)

Figure 7. Simulation results by CEA, CNSC, JNC, and KTH for point B4, located in the buffer at the surface of the waste canister (as shown in Figure 3).



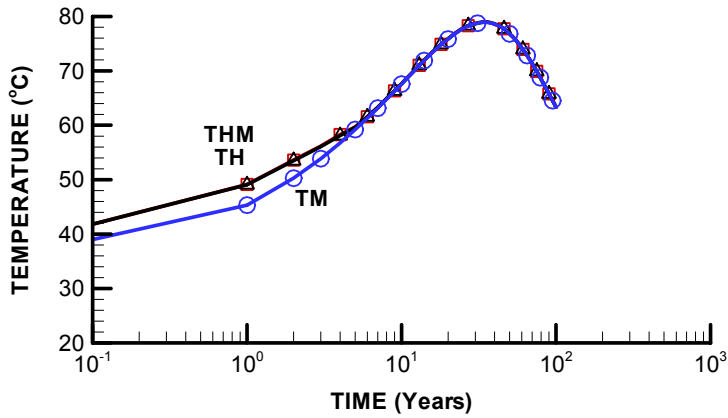
(a) Time evolution of  $\sigma'_1$  and  $\sigma'_3$



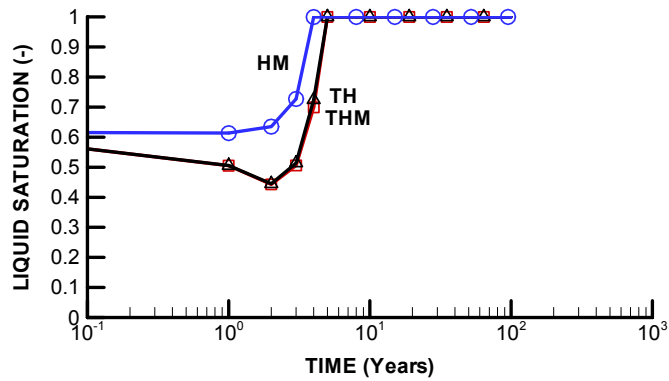
(b) Principal stress path and failure envelop

Figure 8. Simulation results achieved by KTH showing evolution of maximum and minimum principal compressive effective stresses for point R1 located in the rock just below drift floor (as shown in Figure 3). Minimum compressive principal stress is generally oriented normal to the drift floor, whereas maximum compressive principal stress is generally oriented parallel to the drift floor.

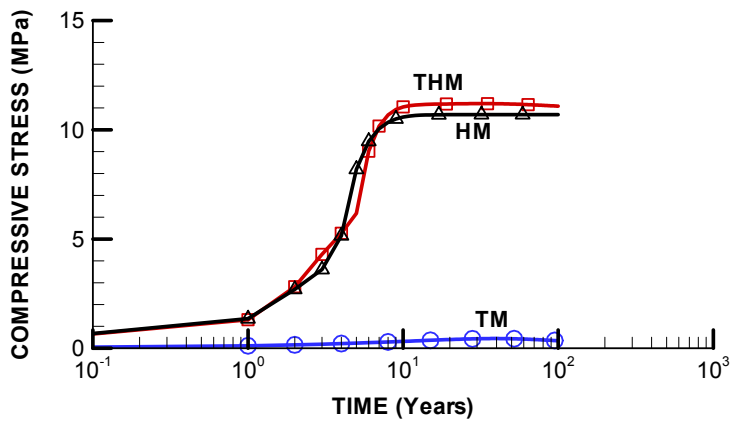




(a) Temperature evolution

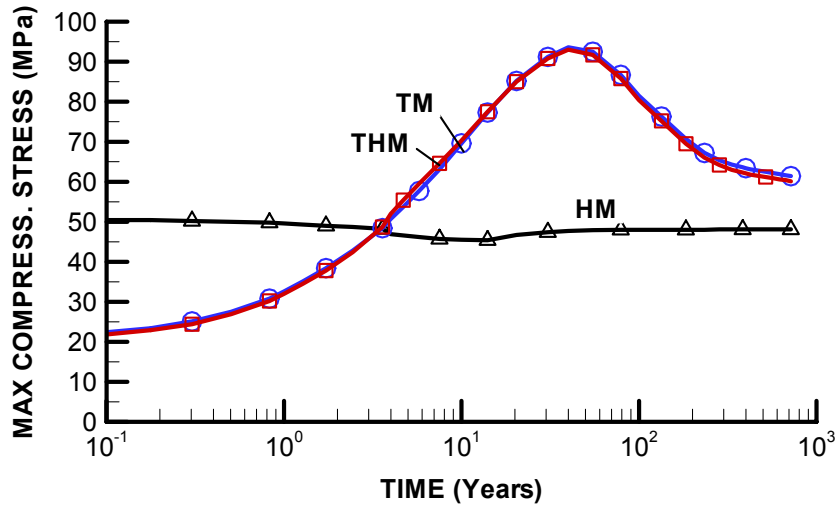


(b) Evolution of liquid saturation

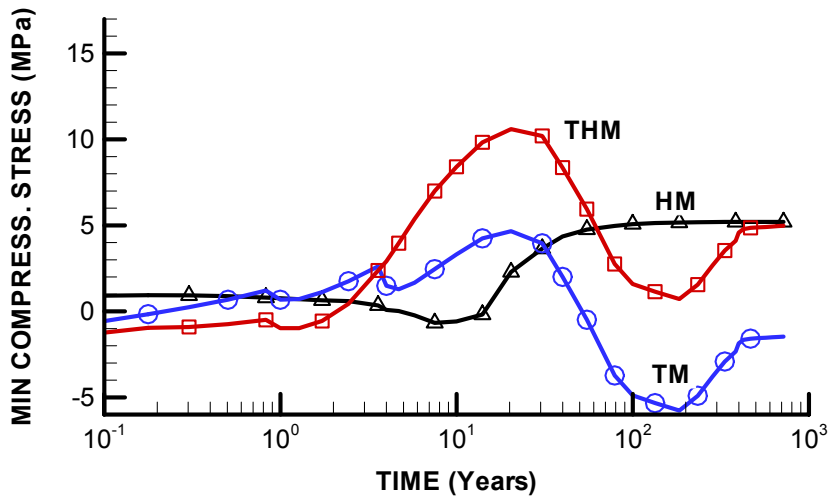


(c) Evolution of compressive stress

Figure 9. Simulation results by CEA showing the impact of HM, TH, TM, and THM coupling for point B4 located in the buffer at the surface of the waste canister (as shown in Figure 3).

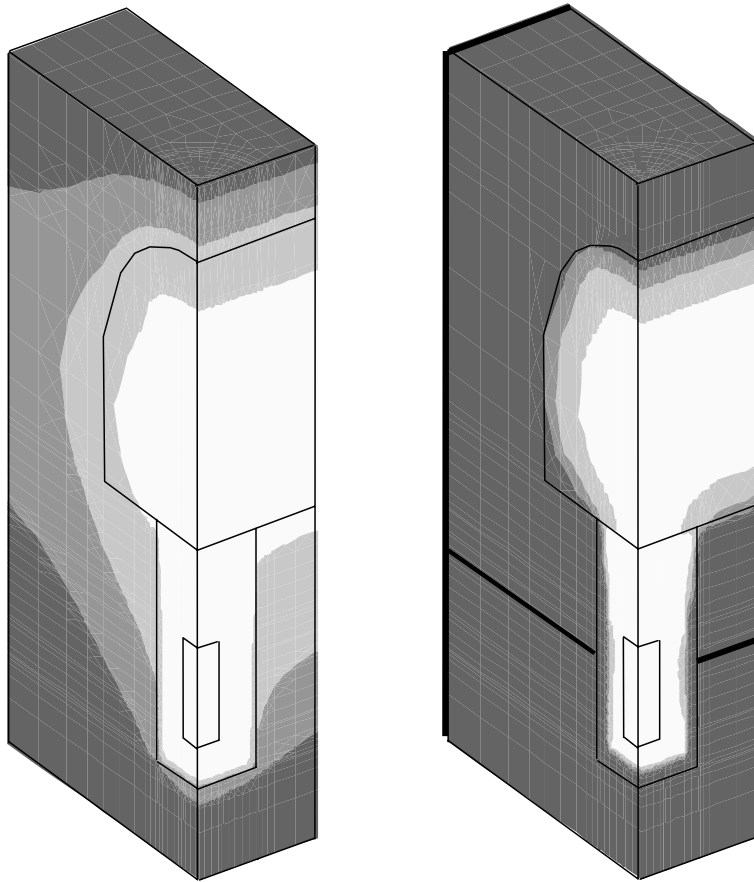


(a) Max compressive principal effective stress



(b) Min compressive principal effective stress

Figure 10. Simulation results achieved by KTH showing the impact of HM, TM, and THM couplings on principal effective stress evolution for point R1 located in the rock just below drift floor (as shown in Figure 3). Minimum compressive principal stress is generally oriented normal to the drift floor, whereas maximum compressive principal stress is generally oriented parallel to the drift floor.



(a) Homogenous intact rock

(b) Sparsely fractured rock

Figure 11. Liquid saturation at 1 year from KTH simulation. Darkest contour indicates fully saturated conditions, whereas lightest contour indicates less than 70% saturation.

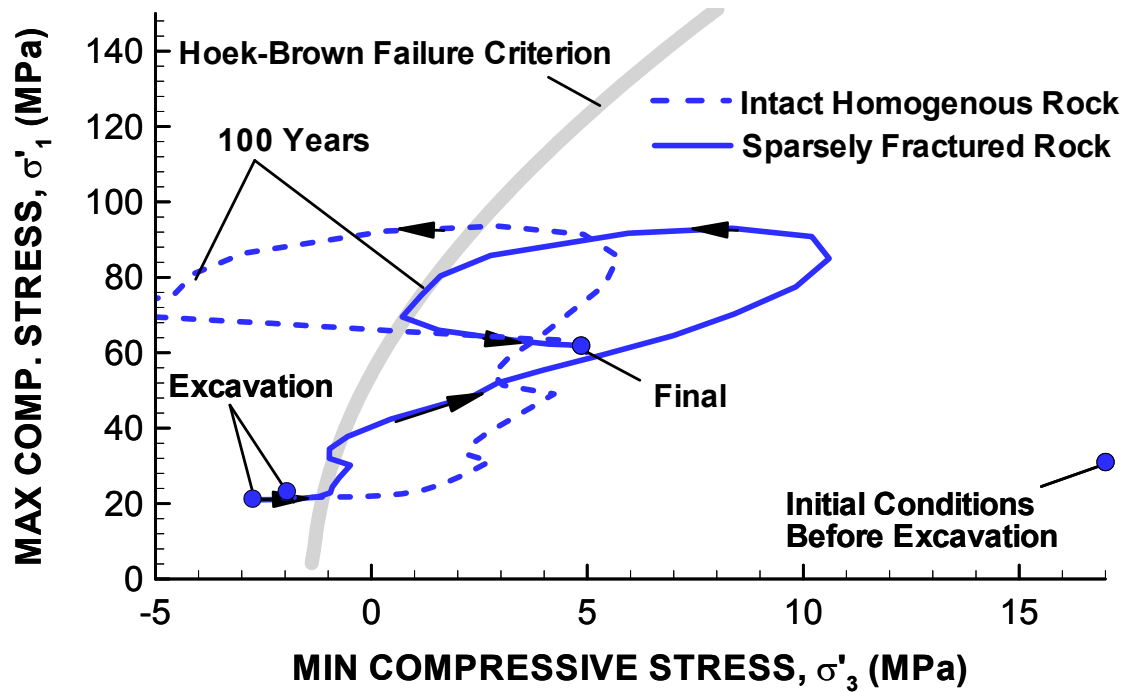


Figure 12. Simulation results achieved by KTH showing evolution of maximum and minimum principal compressive effective stresses for point R1 located in the rock just below drift floor (as shown in Figure 3) for intact homogeneous rock and sparsely fractured rock

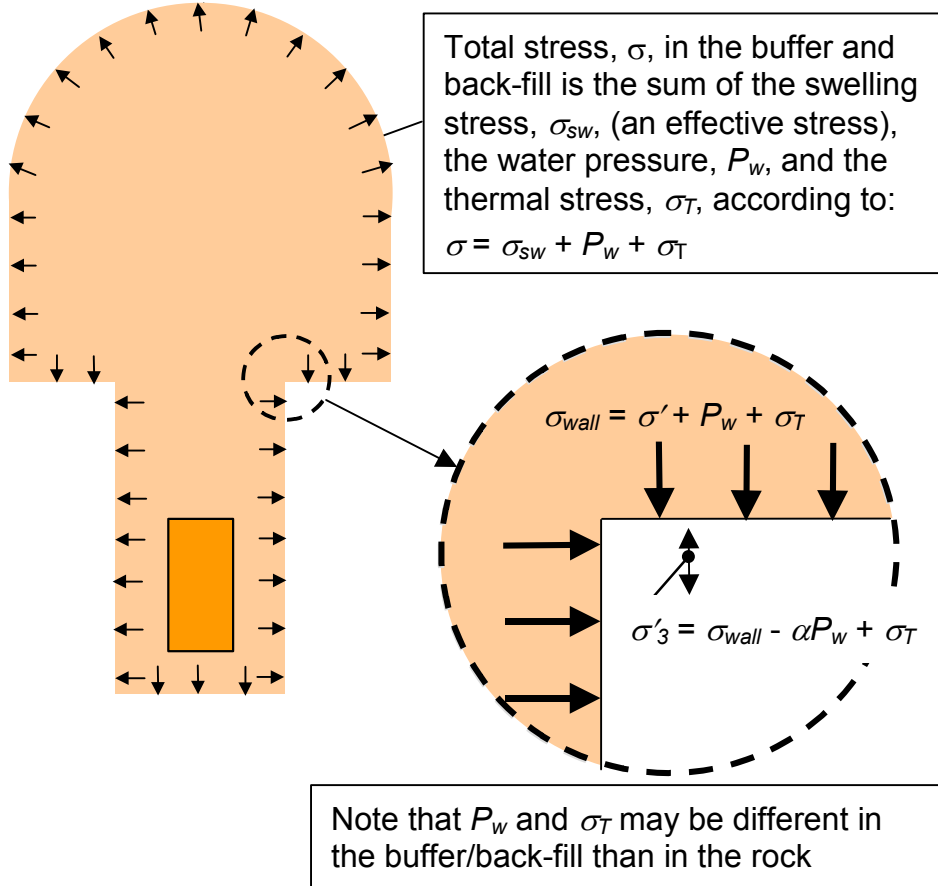


Figure 13. Illustration of the effect of compressive stress,  $\sigma$ , in the back-fill on minimum compressive principal effective stress,  $\sigma'_3$ , in the floor of the drift.